

Cl₂/O₂-inductively coupled plasma etching of deep hole-type photonic crystals in InP

C. F. Carlström,^{a)} R. van der Heijden, F. Karouta,
R. W. van der Heijden, and H. W. M. Salemink^{b)}

COBRA Inter-University Research Institute, Eindhoven University of Technology, P.O. Box 513,
5600 MB Eindhoven, The Netherlands and Center for Nano Materials, Eindhoven University of Technology,
P.O. Box 513, 5600 MB Eindhoven, The Netherlands

E. van der Drift

Kavli Institute of Nanoscience, Delft University of Technology, P.O. Box 5053, 2600 GB Delft,
The Netherlands

(Received 11 March 2005; accepted 21 November 2005; published 25 January 2006)

We have developed an inductively coupled plasma etching process for fabrication of high-aspect-ratio hole-type photonic crystals in InP, which are of interest for optical devices involving the telecommunication wavelength of 1550 nm. The etching was performed at 250 °C using Cl₂/O₂ chemistry for sidewall passivation. The process yields nearly cylindrical features with an aspect ratio larger than 10 for hole diameters near 0.25 μm. This makes them very suitable for high-quality photonic crystal patterns. © 2006 American Vacuum Society.
[DOI: 10.1116/1.2151915]

InP-based two-dimensional hole-type photonic crystals are likely to be present in many of the future optical devices involving the telecommunication wavelength of 1550 nm. For this application, the etched holes are placed on a triangular lattice with a pitch of $a \sim 400$ nm and diameter of $d \sim 250$ nm and etched through an InP/InGaAsP/InP planar waveguide structure. To minimize optical loss, the holes should be ~ 2.5 μm deep and exhibit smooth and vertical sidewalls.¹ Excellent results have been achieved with chemically assisted ion beam etching^{2,3} and electron cyclotron resonance reactive ion etching (RIE) (Ref. 4) using Ar/Cl₂-chemistry. A more versatile technique for large-scale fabrication is inductively coupled plasma (ICP) etching. This technique provides a high etch rate due to high current density and allows independent control of the ion energy. Excellent results on deep-hole etching have already been obtained with ICP using SiCl₄ chemistry.⁵ Here, we present detailed results of successful fabrication of InP photonic crystals by ICP etching, using simple Cl₂ gas to provide the reactive species. In this way, we extend the versatility of Cl₂-based InP device manufacturing.

We have previously reported on ICP etching of hole-type photonic crystals using Cl₂ chemistry.^{6,7} Reasonably deep holes (2.3 μm) could be etched, but with significant undercut in the top region and sloped sidewalls (87°). Since the limited hole depth requires the guiding core layer to be in close vicinity to the top surface these undercut regions may cause significant optical loss.⁸ Our approach to add N₂ to the Cl₂-plasma chemistry resulted in vertical sidewalls with no undercut because of sidewall passivation.⁷ However, the hole

depth was limited to 1 μm due to low etch selectivity with respect to the mask.

An alternative candidate for surface passivation could be O₂. This gas was shown to be very effective in fluorine (SF₆)-based etching of high-aspect-ratio structures in Si.⁹ Furthermore, it has been shown by Smolinsky *et al.*¹⁰ that GaAs etches selectively with respect to oxides in Cl₂ plasma. No selective etching of InP with respect to its oxides was observed in Ref. 10. However, in their case, the etching mechanism was probably rather physical as the substrate temperature (60 °C) was significantly lower than required for chemical etching of InP.¹⁰ Cl₂/O₂ mixtures have indeed been used in reactive ion etching (RIE) of InP laser stripe facets, producing vertical sidewalls at 250 °C.¹¹ In the present article, we demonstrate the feasibility of Cl₂/O₂ ICP etching at temperatures near 250 °C for fabrication of high-aspect-ratio holes needed in photonic crystals.

All experiments were performed on (100) *n*-type InP (Sn-doped) substrates with a size of approximately 8 × 8 mm². The photonic crystal pattern is defined into a layer of ZEP520A (positive electron-beam resist) with electron-beam lithography. This pattern is then transferred into a 400 nm thick, plasma-enhanced chemical vapor deposited SiN_x-masking layer with a RIE process employing CHF₃ as etch gas. After the final ICP etch step, the samples were cleaved and the cross section was inspected with a scanning electron microscope (SEM). The ICP etch experiments were carried out in a load-locked Oxford Plasmalab 100 system. As the main etch product, InCl₃, is not volatile enough at room temperature, all etching was performed at an elevated temperature (250 °C) to ensure chemical etching by Cl.¹² Sample temperature control in ICP etching can be difficult due to significant heating by the ion bombardment.¹³ To keep the sample temperature as close to the preset value as possible, the following measures were taken. The samples were

^{a)}Electronic mail: c.f.c.carlstrom@tue.nl

^{b)}Also at Kavli Institute of Nanoscience, Delft University of Technology, P.O. Box 5053, 2600 GB Delft, The Netherlands.

glued with heat conducting paste onto a 4 in. silicon carrier wafer. The table temperature was regulated by resistive heating in combination with short sequenced processing (etch steps of 30 s) allowing the sample to cool down between the etch steps. Due to the plasma stabilization time of less than 3 s, the sequencing could lead to an underestimate (<10%) of the etch rates. The substrate chuck temperature was measured with a thermocouple. The ion energy was controlled by the dc-bias voltage.

In a first series of experiments, the passivation capabilities of O₂ for the Cl₂ ICP process were investigated. Figure 1(a) illustrates the Cl₂-only case showing a 10 μm wide trench after 1 min (i.e., 2 etch steps) etching using 7 sccm Cl₂ at 2 mTorr with an ICP power of 500 W and dc bias of -500 V. The slight undercut of the vertical sidewalls suggests ion-assisted chemical etching. By adding 1.8 sccm O₂, the sidewalls become more vertical as can be seen in Fig. 1(b). The etch depth for the two processes is comparable: 4.7 μm [Fig. 1(a)] and 4.9 μm [Fig. 1(b)], while the bottom roughness slightly increases [Fig. 1(b)]. However, when the O₂ flow is increased to 2.6 sccm [see Fig. 1(c)], the bottom surface becomes very rough and the etch depth is significantly reduced (~2.5 μm). This grasslike roughness has some darker features on top. These most likely consist of broken grass, clustered together during etching. This is observed more clearly when the O₂ flow is further increased (not shown). Evidently, at higher O₂ flows, the enhanced passivation effect causes micromasking at the bottom surface and inhibits etching despite direct exposure to the ion bombardment. These results indicate that O₂ indeed has a strong passivation effect.

The passivation effect on the sidewalls is even more evident in the case of high-aspect-ratio holes. Figures 2(a) and 2(b) show cross sections of a triangular photonic crystal lattice consisting of 200 nm wide holes and a lattice parameter of 400 nm. Here, the crystals were etched using the process just described with the Cl₂-only, shown in Fig. 2(a), and with the 1.8 sccm O₂ addition, shown in Fig. 2(b). In the Cl₂-only case, the lateral etching in the top region is more pronounced than for the trench [Fig. 1(a)] with openings in the sidewalls to the neighboring holes. The hole bottom profile near the corners shows slight trenching [buckle up shape in Fig. 2(a)], which is indicative for substantial ion impact in the etching process with ions being reflected from the sidewall. In sharp contrast, with addition of O₂ [Fig. 2(b)] the sidewalls are more vertical, although a slight undercut is still visible. The holes in the latter case are deeper and have a rough bottom surface. Apparently, in the Cl₂/O₂ process, etch products collect at the bottom and cause micromasking, which dominates the bottom profile. The bowing in the top [Figs. 1(a) and 2(a)] is well known from deep silicon etching.¹⁴ In that case, it was shown from simulations that the undercut is due to direct exposure of radicals from the plasma in combination with ions scattered from the mask.¹⁴ When O₂ is added, surface passivation protects the sidewalls from etching and chlorine radicals are not consumed there. Consequently, the radicals are available at the bottom surface, which is acti-

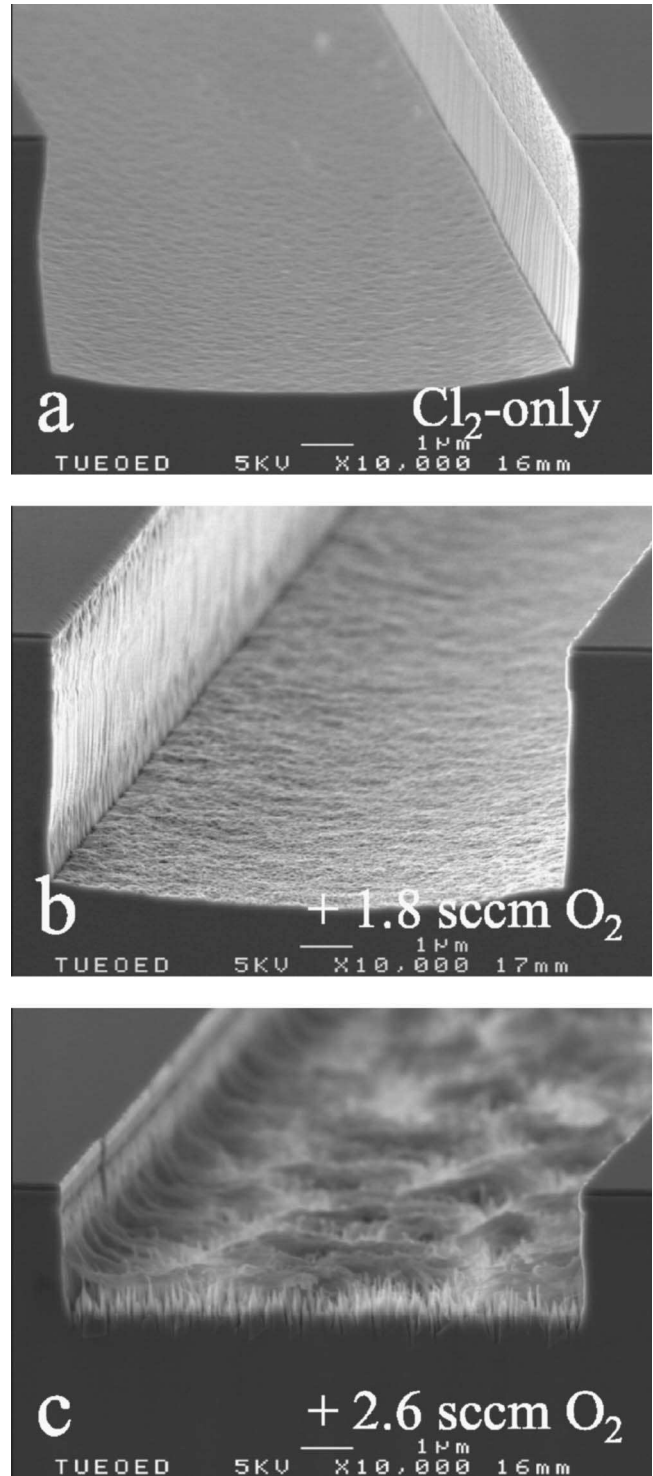


Fig. 1. SEM micrographs of 10 μm wide trenches etched at 2 mTorr and 250 °C using an ICP power of 500 W and dc bias of 500 V. Gas flow rates were (a) 7 sccm Cl₂, (b) 7 sccm Cl₂+1.8 sccm O₂, and (c) 7 sccm Cl₂+2.6 sccm O₂.

vated by the ion bombardment. In this way, a very anisotropic etching process is obtained, leading to large hole depths.

The different etch behavior of large and small areas upon O₂ addition prompted us to perform a more systematic study

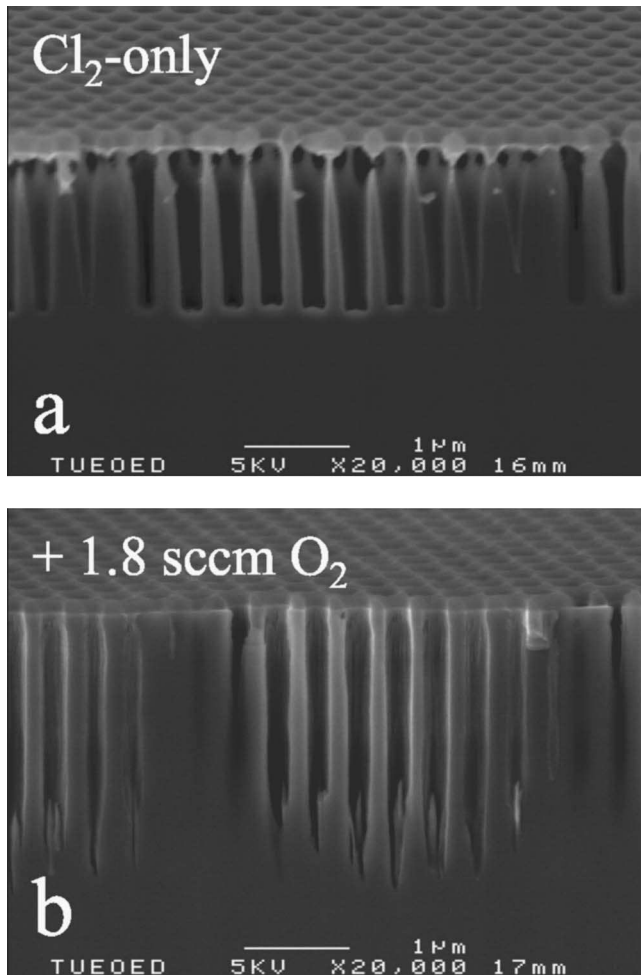


FIG. 2. SEM micrographs of photonic crystals etched at 2 mTorr and 250 °C using an ICP power of 500 W and dc bias of 500 V. Gas flow rates were (a) 7 sccm Cl₂ and (b) 7 sccm Cl₂+1.8 sccm O₂. Note that the photonic crystal symmetry axis (ΓK) makes a small angle ($\sim 5^\circ$) with respect to the cleaving plane, giving a three-dimensional impression of the hole shape.

of aspect-ratio dependent etching (ARDE). Figure 3 summarizes the dependence of etch depth on hole diameter (200, 240, 400, and 960 nm) at different O₂ flows. The Cl₂ flow was 7 sccm while the O₂ flow was 0, 1.8, 2.6, or 7 sccm. For comparison, the etch depth of the 10 μ m wide trench is also included. In the Cl₂-only case, the etch depth decreases with decreasing hole diameter, also known as RIE-lag. When increasing the amount of O₂, the RIE-lag is reduced; eventually leading to inverse RIE-lag (etch depth increase with decreasing hole diameter) at the largest O₂ flow. The consequences of O₂ addition for the overall etch behavior with respect to ARDE are twofold, each with a different impact. On the one hand improved sidewall passivation leads to enhanced exposure of the bottom to reactive species, which will increase the etch rate. On the other hand, improved bottom passivation inevitably leads to lower etch rates due to formation of less volatile etch products. The results in Fig. 3 indicate that the resultant of the two effects varies largely with aspect ratio. In the lower aspect ratio regime (960 nm diameter hole, 10 μ m trench) the enhanced

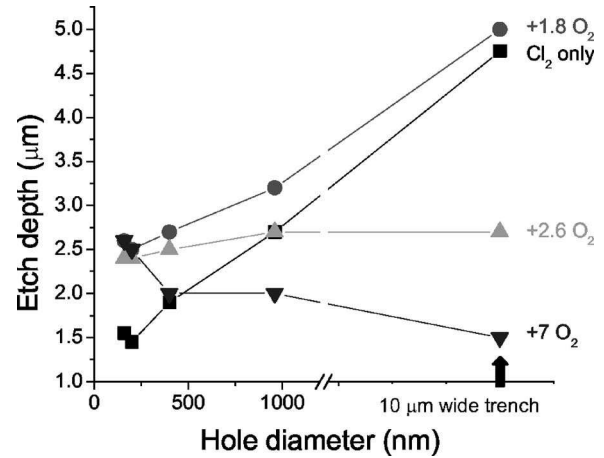


FIG. 3. Etch depth as a function of hole diameter for photonic crystal holes after 1 min etching at 2 mTorr and 250 °C using a Cl₂/O₂ mixture with 7 sccm Cl₂. ICP power and dc bias were 250 W and 640 V.

bottom passivation and slow down of the etch rate dominates for increasing O₂ content after a slight increase at the lowest O₂ addition (1.8 sccm). In the high-aspect-ratio regime (200 and 240 nm diameter), the impact of sidewall passivation and the correspondingly enhanced flux of reactive species to the bottom dominates. The hole depth is independent of the given O₂-flow range. Apparently, the bottom surface is hardly passivated in these high-aspect-ratio holes at this flow regime. The same etch behavior is also observed using a higher Cl₂ flow of 14 sccm (not shown), but then the hole depth is significantly larger. The abundance of neutral species at the hole bottom is strongly dependent on aspect ratio.¹⁵ Evidently, in this regime the ion-enhanced etching is limited by the supply of neutral Cl species. It is pointed out that with a proper Cl₂/O₂ balance, the etching process can be tuned to aspect *independent* etching, as manifested by the 2.6 sccm O₂ curve in Fig. 3. This could be very useful when the waveguide and photonic crystal element are to be realized in a single etch step. Apart from all surface chemical effects at the sidewall and bottom, the addition of oxygen increases the dissociation¹⁶ and ionization of chlorine since the strong electron attachment mechanism for chlorine will be suppressed. The systematic increase of the etch depth when 1.8 sccm of O₂ is added could be partly ascribed to this effect.

From the above discussion it is clear, that a Cl₂/O₂ balance is crucial not only with respect to pressure and temperature to control the flux of Cl radicals, but also with respect to the ICP and chuck bias powers as these parameters affect the dissociation/ionization ratio and the ion energy, respectively. Figures 4(a) and 4(b) show cross sections of photonic crystal structures after 1 min of etching using more optimized conditions. Here, the pressure was 2 mTorr and the gas flows were set to 14 sccm and 1.8 sccm for Cl₂ and O₂, respectively. The ICP power was lowered (250 W) and the dc bias increased (640 V). The holes in Fig. 4(a) are of typical size for the photonic crystals operating at 1.55 μ m (vacuum wavelength), being 240 nm in diameter and on a pitch of

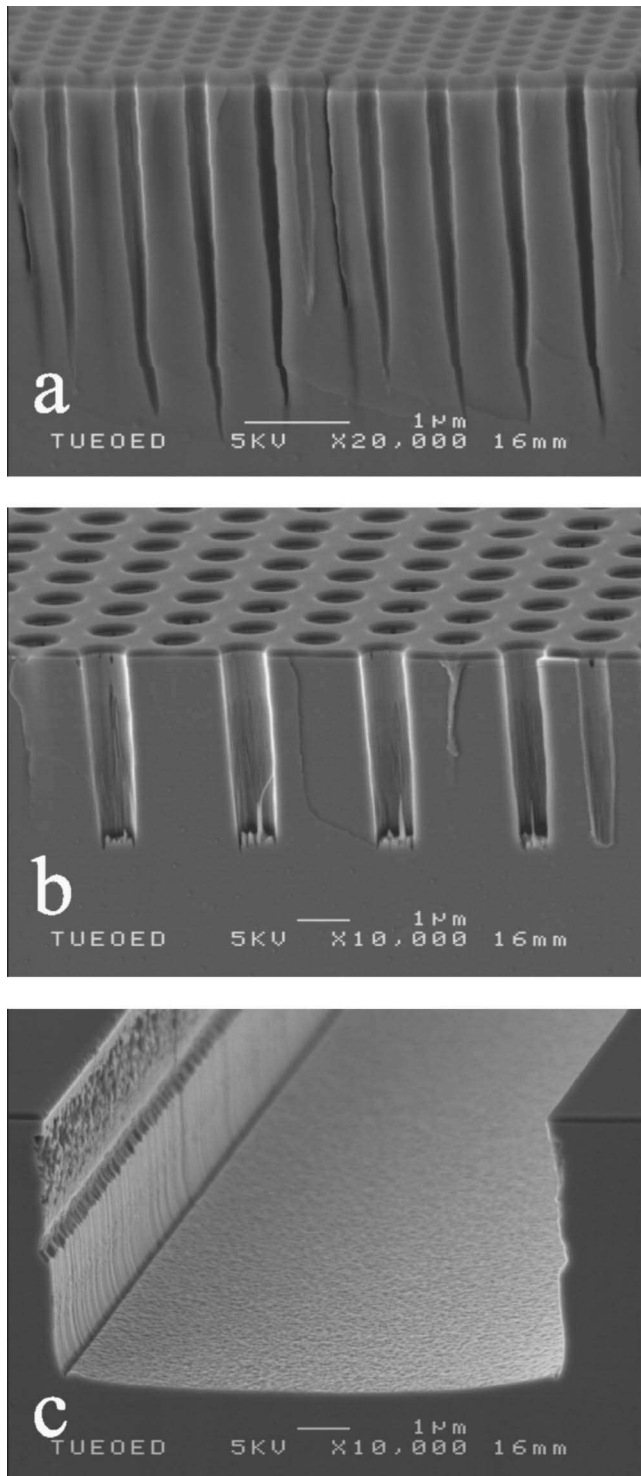


FIG. 4. SEM micrographs of photonic crystal holes and a trench. The etching was carried out at 2 mTorr and 250 °C using an ICP power of 250 W and dc bias of 640 V. Gas flow rates were 14 sccm Cl₂+1.8 sccm O₂: (a) Hole diameter 240 nm, (b) hole diameter 960 nm, and (c) trench width 10 μm.

400 nm. The holes are deep (~3.4 μm) and, more important for hole-type photonic crystal applications, the sidewalls are almost vertical (>89°) in the upper 2 μm. At this low ICP power, the bottom part of the high-aspect holes is narrow, which appears to be a commonly encountered feature in InP

photonic crystal etching.²⁻⁵ The narrowing might relate to shadowing of ions and/or neutrals. Similarly, the wider holes of 960 nm [Fig. 4(b)] and 480 nm (not shown) in diameter also have a cylindrical shape in their upper part. The micro-masking of these holes [Figs. 4(a) and 4(b)] is either absent or occurs at a lesser extent [compared to Fig. 2(b)] probably due to a lower oxygen fraction, i.e., 14/1.8 compared to 7/1.8. The sidewall surface exhibits some striations in the upper region, most likely originating from the mask. For the trench, depicted in Fig. 4(c), the whole upper region of the sidewall is very rough and there is a marked transition to the smoother lower region. Similar abrupt transitions in sidewall roughness have been observed before with other dry etching processes, including Cl₂/O₂-RIE and has been attributed to the redeposition of nonvolatile etch products.^{11,17} We observe this transition also in the Cl₂-only case, though it is then less pronounced [Fig. 1(a)].

In summary, we have demonstrated that O₂ is capable of surface passivation in Cl₂-based ICP etching of InP and that the balance of neutral and ionic species is crucial. While work on optimizing this process to obtain smooth and vertical sidewalls for both low and high-aspect-ratio features is still in progress, these first results show that this process is very suitable for fabrication of deep hole photonic crystals structures in InP.

The authors would like to thank E. J. Geluk and P. Nouwens for technical assistance. Part of this research is supported by NanoNed, a technology programme of the Dutch Ministry of Economic Affairs.

- ¹R. Ferrini, R. Houdré, H. Benisty, M. Qiu, and J. Moosburger, *J. Opt. Soc. Am. B* **20**, 469 (2003).
- ²M. V. Kotlyar, T. Karle, M. D. Settle, L. O'Faolain, and T. F. Krauss, *Appl. Phys. Lett.* **84**, 3588 (2004).
- ³M. Mulot, S. Anand, R. Ferrini, B. Wild, R. Houdré, J. Moosburger, and A. Forchel, *J. Vac. Sci. Technol. B* **22**, 707 (2004).
- ⁴T. D. Happ, A. Markard, M. Kamp, A. Forchel, S. Anand, J. L. Gentner, and N. Bouadma, *J. Vac. Sci. Technol. B* **19**, 2775 (2001).
- ⁵F. Pommereau, L. Legouezigou, S. Hubert, S. Sainson, J. P. Chandouineau, S. Fabre, G. H. Duan, B. Lombardet, R. Ferrini, and R. Houdre, *J. Appl. Phys.* **95**, 2242 (2004).
- ⁶R. van der Heijden, M. S. P. Andriess, C. F. Carlström, E. van der Drift, E. J. Geluk, R. W. van der Heijden, F. Karouta, P. Nouwens, Y. S. Oei, T. de Vries, and H. W. M. Salemink, *Proc. SPIE* **5450**, 523 (2004).
- ⁷R. van der Heijden, C. F. Carlström, M. S. P. Andriess, E. van der Drift, E. J. Geluk, R. W. van der Heijden, F. Karouta, P. Nouwens, Y. S. Oei, T. de Vries, and H. W. M. Salemink, in *Proceedings of the Symposium IEEE/LEOS Benelux Chapter* (Ghent, Belgium, 2004), p. 287.
- ⁸R. Ferrini, A. Berrier, L. A. Dunbar, R. Houdré, M. Mulot, S. Anand, S. de Rossi, and A. Talneau, *Appl. Phys. Lett.* **85**, 3998 (2004).
- ⁹T. Zijlstra, E. van der Drift, M. J. A. de Dood, E. Snoeks, and A. Polman, *J. Vac. Sci. Technol. B* **17**, 2734 (1999).
- ¹⁰G. Smolinsky, R. P. Chang, and T. M. Mayer, *J. Vac. Sci. Technol.* **18**, 12 (1981).
- ¹¹L. A. Coldren and J. A. Rentschler, *J. Vac. Sci. Technol.* **19**, 225 (1981).
- ¹²S. C. McNevin, *J. Vac. Sci. Technol. B* **4**, 1216 (1986).
- ¹³E. Sabin, *J. Vac. Sci. Technol. B* **16**, 1841 (1998).
- ¹⁴G. Marcos and A. Rhallabi, *J. Vac. Sci. Technol. B* **21**, 87 (2002).
- ¹⁵J. W. Coburn and H. F. Winters, *Appl. Phys. Lett.* **55**, 2730 (1989).
- ¹⁶R. H. Burton and G. Smolinsky, *J. Electrochem. Soc.* **129**, 1599 (1982).
- ¹⁷C. Youtsey, R. Grundbacher, R. Panepucci, I. Adesida, and C. Caneau, *J. Vac. Sci. Technol. B* **12**, 3317 (1994).